DOI: 10.17344/acsi.2024.8763 *Acta Chim. Slov.* **2024,** *71,* 462–470

Scientific paper

Synthesis, Crystal Structures and Antibacterial Activity of Nickel(II), Cadmium(II) and Zinc(II) Complexes with Hydrazone Ligands

Wei-Guang Zhang

College of Chemistry and Chemical Engineering, Qiqihar University, Qiqihar 161006, P. R. China

** Corresponding author: E-mail: zhangweiguang1230@163.com*

Received: 04-11-2024

Abstract

Three mononuclear nickel(II), cadmium(II) and zinc(II) complexes, $[NiL_2]\cdot 2CH_3OH\cdot H_2O$ (**1**), $[CdI_2(HL)]\cdot CH_3OH$ (**2**) and $[ZnL_2]$ (**3**), have been synthesized from 3-hydroxy-4-methoxy-*N*'-[(*Z*)-(pyridin-2-yl)methylidene]benzohydrazide (HL) by microwave irradiation method. All complexes were characterized by CHN elemental analyses and infrared spectra. Structures of the complexes were further studied by single crystal X-ray determination, which reveals that the Ni and Zn atoms in complexes **1** and **3** are in octahedral coordination, and the Cd atom in complex **2** is in square pyramidal coordination. The biological activity of the complexes on the bacterial strains *Bacillus subtilis*, *Staphylococcus aureus*, *Pseudomonas aeruginosa* and *Escherichia coli* was evaluated. As a result, the zinc complex has interesting antibacterial activities.

Keywords: Hydrazone; nickel complex; cadmium complex; zinc complex; antibacterial activity

1. Introduction

Microwave-assisted synthesis of various organic and coordination compounds has received much attention in recent years because it can accelerate their reactions.[1] In addition, this method has obvious advantages in providing a cheap, clean and easy handling heating way in the synthesis of various types of compounds with higher yields and less reaction time by comparing with those heating at reflux in organic solvents or solvothermal method.[2] Till date, microwave irradiation is considered to be one of the robust and efficient techniques for the synthesis of Schiff base metal complexes. The greatest advantage of this technique is the extraordinary acceleration in reaction rate when compared to conventional method.[3] Hydrazones can be prepared by reaction of aldehydes and aroylhydrazines. They and their metal complexes have various biological activities such as antibacterial,[4] anticancer,[5] antitubercular,[6] as well as enzyme inhibition.[7] When bioorganic molecules or drugs are bound to metal ions, there is drastic enhance in their biomimetic properties, therapeutic effects and pharmacological properties.[8] Orojloo and coworkers reported some cobalt(II), nickel(II), copper(II) and zinc(II) complexes derived from the Schiff base ligands 4-((2,4-dichlorophenyl)diazenyl)-2-(3-hydroxypropylimino)methyl)phenol and 2-((3-hydroxypropylimino)methyl)-4-(thiazol-2 yldiazenyl)phenol. As a result, the complexes have higher activities as compared with the free Schiff bases.[9] Nickel, cadmium and zinc complexes are reported to be biological active like antimicrobial, anticancer, antioxidant, and DNA binding properties.[10] As a continuation of our work on metal complexes with biological activities,[11] in this study, the synthesis, characterization and antibacterial properties of three new complexes $[NiL_2]\cdot 2CH_3OH\cdot H_2O$ (**1**), $[CdI_2(HL)]\cdot CH_3OH$ (**2**) and $[ZnL_2]$ (**3**), derived from 3-hydroxy-4-methoxy-*N*'-[(*Z*)-(pyridin-2-yl)methylidene] benzohydrazide (HL), are presented.

2. Experimental

2. 1. Materials and Physical Methods

Pyridine-2-carboxaldehyde, 3-hydroxyl-4-methoxybenzohydrazide, nickel acetate, cadmium iodide, and zinc acetate were obtained from TCI. The solvents were of AR grade and used as received. The microwave synthesis was carried out with a WX-4000 microwave digestion system. CHN elemental analyses were performed on a Perkin-Elmer 2400 Elemental Analyzer. Infrared spectra were recorded on a Bio-Rad FTS 135 spectrophotometer with KBr pellets.

X-ray single crystal structure diffraction was determined with a Bruker Smart 1000 CCD diffractometer.

2. 2. Synthesis of HL

Pyridine-2-carboxaldehyde (0.11 g, 1.0 mmol) and 3-hydroxyl-4-methoxybenzohydrazide (0.18 g, 1.0 mmol) were mixed in methanol, and stirred at reflux for 30 min. The reaction mixture was evaporated to give colorless solid, which was recrystallized from methanol to give crystalline product. Yield: 0.24 g (89%). Anal. Calcd. for $C_{14}H_{13}N_3O_3$ (%): C, 61.99; H, 4.83; N, 15.49. Found (%): C, 62.23; H, 4.90; N, 15.37. IR data (KBr, cm^{-1}): 3308, 3272, 1684, 1621, 1569, 1507, 1461, 1425, 1331, 1305, 1273, 1232, 1145, 1113, 1029, 885, 843, 817, 760, 713, 646, 578. ^{1}H NMR (500 MHz, d_6-DMSO): δ 9.49 (s, 1H, OH), 9.12 (s, 1H, NH), 8.63 (d, 1H, PyH), 7.87 (d, 1H, PyH), 7.81 (t, 1H, PyH), 7.60 (t, 1H, PyH), 7.45 (s, 1H, CH=N), 7.29 (m, 2H, ArH), 6.95 (d, 1H, ArH), 3.85 (s, 3H, CH_3). ^{13}C NMR (126 MHz, d_6-DMSO): δ 165.8, 153.2, 150.0, 148.7, 145.9, 144.3, 136.2, 128.1, 126.7, 125.6, 121.3, 120.1, 115.3, 55.6.

2. 3. Synthesis of the Complexes

The three complexes were prepared with the same method as described. Pyridine-2-carboxaldehyde (0.11 g, 1.0 mmol), 3-hydroxyl-4-methoxybenzohydrazide (0.18 g, 1.0 mmol), methanol (30 mL) and metal salts (1.0 mmol as follows) were placed in a Teflon-lined autoclave (30 mL). The reaction mixture was maintained at 350 K and 200 W for 10 min at the cavity of the microwave reactor. Then the reaction mixture was cooled to room temperature for about 60 min. The mixtures were filtered and with the filtrate to slow evaporate in air for a week. Well shaped single crystals were formed and collected by filtration and washed with cold methanol.

2. 3. 1. $[NiL_2]\cdot 2CH_3OH\cdot H_2O$ (1)

Nickel acetate tetrahydrate (0.25 g, 1.0 mmol). Yield: 0.22 g (65%). Anal. Calcd. for $C_{30}H_{34}N_6NiO_9$ (%): C, 52.89; H, 5.03; N, 12.34. Found (%): C, 52.73; H, 5.10; N, 12.17. IR data (KBr, cm^{-1}): 1605, 1561, 1517, 1489, 1460, 1423, 1365, 1351, 1328, 1268, 1243, 1217, 1180, 1134, 1118, 1072, 1015, 971, 878, 855, 820, 765, 680, 643, 599, 555, 518, 493.

2. 3. 2. $[CdI_2(HL)]\cdot CH_3OH$ (2)

Cadmium iodide (0.37 g, 1.0 mmol). Yield: 0.41 g (61%). Anal. Calcd. for $C_{15}H_{17}CdI_2N_3O_4$ (%): C, 26.91; H, 2.56; N, 6.28. Found (%): C, 27.05; H, 2.47; N, 6.22. IR data (KBr, cm^{-1}): 1628, 1614, 1580, 1550, 1508, 1473, 1441, 1358, 1293, 1229, 1212, 1146, 1125, 1083, 1010, 968, 878, 827, 783, 767, 747, 638, 576, 532, 507, 472.

2. 3. 3. $[ZnL_2]$ (3)

Zinc acetate dihydrate (0.22 g, 1.0 mmol). Yield: 0.23 g (74%). Anal. Calcd. for $C_{28}H_{24}N_6O_6Zn$ (%): C, 55.50; H,

Table 1. Crystallographic data for the complexes

Complex	1	2	3
Formula	$C_{30}H_{34}N_6NiO_9$	$C_{15}H_{17}CdI_2N_3O_4$	$C_{28}H_{24}N_6O_6Zn$
Formula weight	681.34	669.52	605.90
Crystal system	Orthorhombic	Monoclinic	Triclinic
Space group	*Pbca*	$P2_1/c$	*P*-1
a (Å)	15.1673(10)	8.3494(13)	8.4352(10)
b (Å)	19.8159(10)	14.3589(15)	11.4227(11)
c (Å)	20.9173(13)	17.4204(13)	14.7073(15)
α (°)	90	90	88.9880(10)
β (°)	90	95.9160(10)	77.2480(10)
γ (°)	90	90	74.8700(10)
V (Å^3)	6286.8(7)	2077.4(4)	1333.0(2)
λ (Å)	0.71073	0.71073	0.71073
ρ_{calcd} (g cm^{-3})	1.440	2.141	1.510
Z	8	4	2
μ (mm^{-1})	0.680	4.046	0.977
θ ranges (°)	1.95–25.50	1.84–25.50	2.28–25.50
Reflections collected	32240	11012	13780
Independent reflections	5852	3868	4953
Observed reflections ($I \geq 2\sigma(I)$)	3587	2927	2871
Restraints	25	2	2
Parameters	437	234	380
Goodness-of-fit on F^2	1.027	1.039	1.018
Final *R* indices [$I \geq 2\sigma(I)$]	0.0500, 0.1057	0.0321, 0.0607	0.0586, 0.1283
R indices (all data)	0.1028, 0.1293	0.0491, 0.0673	0.1180, 0.1513

3.99; N, 13.87. Found (%): C, 55.28; H, 4.07; N, 13.96. IR data (KBr, cm^{-1}): 1605, 1563, 1515, 1489, 1462, 1420, 1356, 1270, 1241, 1215, 1178, 1137, 1118, 1072, 1028, 1014, 973, 929, 878, 853, 818, 763, 680, 641, 601, 556, 516, 488, 438.

2. 4. X-Ray Structure Determination

X-ray single crystal diffraction was performed on a diffractometer equipped with a graphite monochromated Mo-Kα radiation (λ = 0.71073 Å) at 298(2) K. The collected data were integrated and reduced with SAINT.[12] Structures of the five complexes were solved by direct methods and refined by full-matrix least-squares based on F^2 with SHELXL.[13] The empirical absorption correction was applied with SADABS.[14] All non-H atoms were anisotropically refined. The H atoms attached to O and N atoms in the complexes were located from difference Fourier maps and refined isotropically, with O–H, N–H and H···H distances restrained to 0.85(1), 0.90(1) and 1.37(2) Å, respectively. Selected crystal data for the complexes are summarized in Table 1. Coordinate bond lengths and bond angles are provided in Table 2.

Table 2. Selected bond distances (Å) and bond angles (°) for the complexes

		1	
Ni1–O1	2.119(3)	Ni1–O2	2.067(3)
Ni1–N2	1.974(3)	Ni1–N3	2.109(3)
Ni1–N5	1.971(3)	Ni1–N6	2.117(3)
N5–Ni1–N2	177.72(13)	N5–Ni1–O2	76.66(11)
N2–Ni1–O2	101.20(12)	N5–Ni1–N3	102.44(13)
N2–Ni1–N3	78.30(13)	O2–Ni1–N3	91.06(12)
N5–Ni1–N6	78.28(13)	N2–Ni1–N6	103.84(13)
O2–Ni1–N6	154.94(12)	N3–Ni1–N6	94.95(13)
N5–Ni1–O1	103.53(12)	N2–Ni1–O1	75.69(12)
O2–Ni1–O1	93.67(10)	N3–Ni1–O1	154.00(12)
N6–Ni1–O1	91.51(11)		
		2	
Cd1–I1	2.7147(5)	Cd1–I2	2.7441(6)
Cd1–O1	2.445(3)	Cd1–N2	2.335(4)
Cd1–N3	2.383(4)		
N2–Cd1–N3	69.28(13)	N2–Cd1–O1	65.69(12)
N3–Cd1–O1	134.54(12)	N2–Cd1–I1	125.52(9)
N3–Cd1–I1	104.39(9)	O1–Cd1–I1	96.59(8)
N2–Cd1–I2	115.26(9)	N3–Cd1–I2	103.18(9)
O1–Cd1–I2	101.12(9)	I1–Cd1–I2	118.695(18)
		3	
Zn1–O1	2.207(3)	Zn1–O2	2.141(3)
Zn1–N2	2.067(4)	Zn1–N3	2.219(4)
Zn1–N5	2.052(4)	Zn1–N6	2.291(4)
N5–Zn1–N2	177.60(16)	N5–Zn1–O2	74.66(14)
N2–Zn1–O2	106.23(14)	N5–Zn1–O1	105.27(13)
N2–Zn1–O1	72.42(14)	O2–Zn1–O1	100.22(13)
N5–Zn1–N3	106.92(15)	N2–Zn1–N3	75.27(16)
O2–Zn1–N3	96.50(14)	O1–Zn1–N3	146.64(14)
N5–Zn1–N6	74.60(15)	N2–Zn1–N6	104.71(15)
O2–Zn1–N6	148.77(14)	O1–Zn1–N6	92.99(13)
N3–Zn1–N6	87.25(15)		

2. 5. Antibacterial Assay

The hydrazone HL and the three complexes were assayed *in vitro* antibacterial activities against two Gram-positive bacteria strains *Staphylococcus aureus* and *Bacillus subtilis*, and two Gram-negative bacteria strains *Escherichia coli* and *Pseudomonas aeruginosa* by agar well diffusion method with the literature method.[15] The negative and positive references are DMSO and Ciprofloxacin, respectively.

2. 6. Determination of Minimum Inhibitory Concentration (MIC)

MIC values of the compounds was tested through a modified agar well diffusion method.[16] A two-fold serial dilution of each compound was prepared by first reconstituting in DMSO followed by dilution in sterile distilled water to achieve a decreasing concentration range 256 μM. Each dilution (100 μL) was introduced into wells in the agar plates seeded with 100 μL of standardized inoculums (10^6 cfu mL^{-1}) of the microbial strain. All test plates were incubated aerobically at 37 °C for 24 h and observed for the inhibition zones.

3. Results and Discussion

3. 1. Chemistry

Reaction of in situ formed HL with nickel acetate (for **1**), cadmium iodide (for **2**) and zinc acetate (for **3**), respectively, afforded the complexes (Scheme 1).

3. 2. IR Spectra

In the IR spectra of complexes **1** and **3**, the characteristic imine stretching is observed at 1605 cm^{-1} as strong signals.[17] In complex **2**, the imine stretching is observed at 1614 cm^{-1}. This is in agreement with the different lengths of C=N bonds in these complexes. There is an obvious strong absorption at 1628 cm^{-1} in the spectrum of complex **2**, while absence in the other two complexes, which is assigned to C=O vibration.[18] Coordination of the ligands is further confirmed by the appearance of weak bands in the low wave numbers 400–600 cm^{-1}, corresponding to ν(M–N), ν(M–O) and ν(M–I).[19]

3. 3. Structure Description of Complex 1

The molecular structure of complex **1** is shown in Fig. 1. The compound contains a mononuclear [NiL_2] complex molecule, and one water and two methanol molecules of crystallization. The Ni atom is coordinated by two pyri-

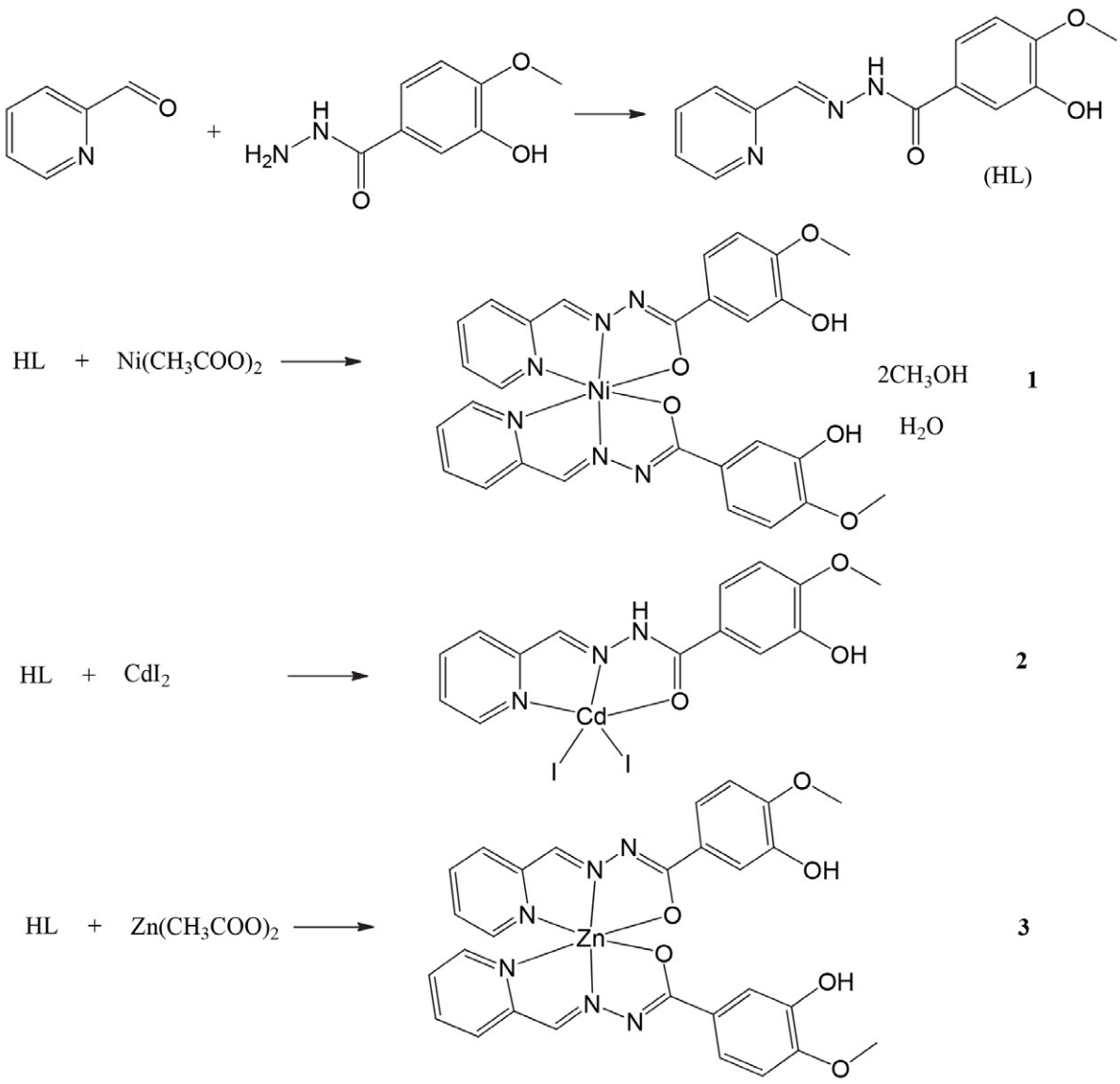

Scheme 1. The synthetic procedure for HL and the complexes.

dine nitrogens (N3, N6), two imino nitrogens (N2, N5), and two enolate oxygens (O1, O2) from two hydrazone ligands, forming octahedral geometry. The octahedral coordination is distorted from the ideal model, which can be evidenced by the bond angles, ranging from 75.69(12) to 103.84(13)° for the *cis* angles, and from 154.00(12) to 177.72(13)° for the *trans* angles. The distortion arises from the strain created by the four five-membered chelate rings. The lengths of Ni–O bonds (2.067(3)-2.119(3) Å) and Zn–N bonds (1.971(3)-2.117(3) Å) are comparable to those observed in Schiff base nickel complexes with octahedral coordination.[20] The C1-C6 benzene ring and the C9-C13-N3 pyridine ring form a dihedral angle of 19.6(5)°. The C15-C20 benzene ring and the C23-C27-N6 pyridine ring form a dihedral angle of 2.3(5)°. In the crystal structure, the complex molecules and the solvent molecules are linked through intermolecular hydrogen bonds

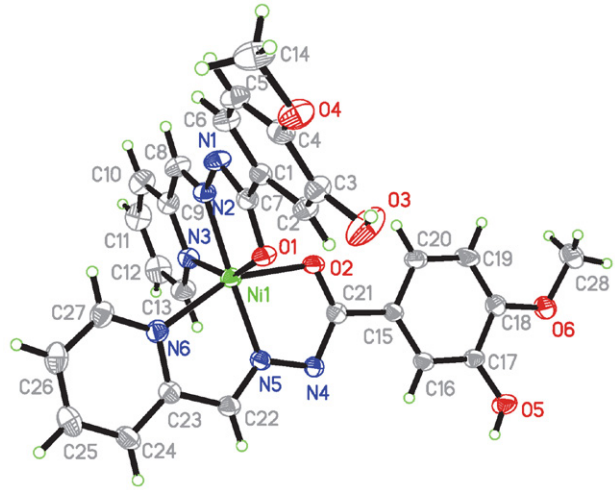

Fig. 1. Molecular structure of complex **1**. Displacement ellipsoids are drawn at the 30% probability level. The solvent molecules are omitted for clarity.

of O–H···N, O–H···O and C–H···O, to form a three-dimensional network (Fig. 2).

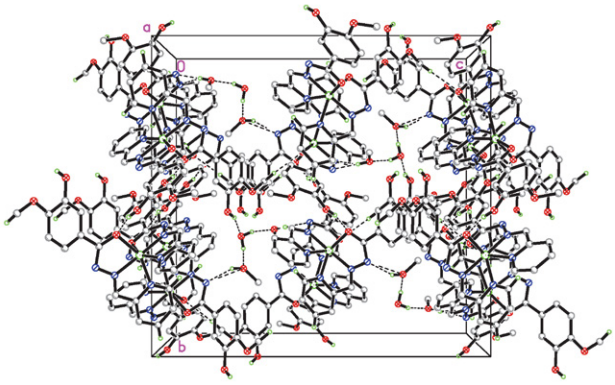

Fig. 2. Molecular packing diagram of complex **1**, viewed along the *a* axis. Hydrogen bonds are shown as dashed lines. H atoms not involved in hydrogen bonding are omitted for clarity.

3. 4. Structure Description of Complex 2

The molecular structure of complex **2** is shown in Fig. 3. The compound contains a mononuclear $[CdI_2(HL)]$ complex molecule and a methanol molecule of crystallization. The Cd atom is coordinated by one pyridine nitrogen (N3), one imino nitrogen (N2), and one carbonyl oxygen (O1) of a hydrazone ligand, and two I ligands (I1, I2), forming square pyramidal geometry. The basal plane is defined by N2, N3, O1 and I1 atoms, and the apical position is occupied by I2 atom. The square pyramidal coordination is distorted from the ideal model, which can be evidenced by the bond angles. The angles in the basal plane are range from 65.69(12) to 104.39(9)° for *cis* angles and from 125.52(9) to 134.54(12)° for *trans* angles. The angles among the apical and basal donor atoms are 101.12(9)-118.695(18)°. The distortion arises from the strain created by the two five-membered chelate rings. The square pyramidal geometry is evidenced by the index value τ of 0.15.[21] The lengths of Cd-O bond (2.445(3) Å) and Cd-N bonds (2.335(4)-2.383(4) Å) are comparable to those observed in Schiff base cadmium complexes.[22] The

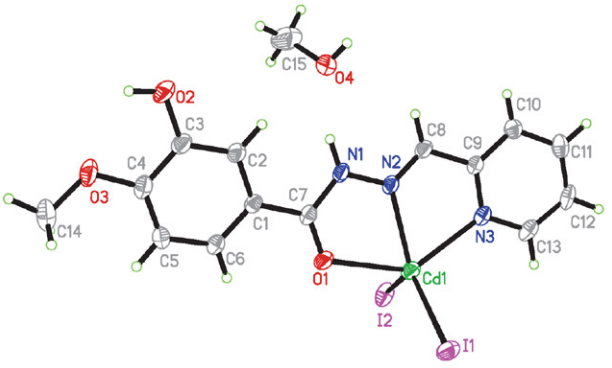

Fig. 3. Molecular structure of complex **2**. Displacement ellipsoids are drawn at the 30% probability level.

C1-C6 benzene ring and the C9-C13-N3 pyridine ring form a dihedral angle of 11.1(3)°. In the crystal structure, the complex molecules and the solvent molecules are linked through intermolecular hydrogen bonds of N–H···O, O–H···O and O–H···I, to form a three-dimensional network (Fig. 4).

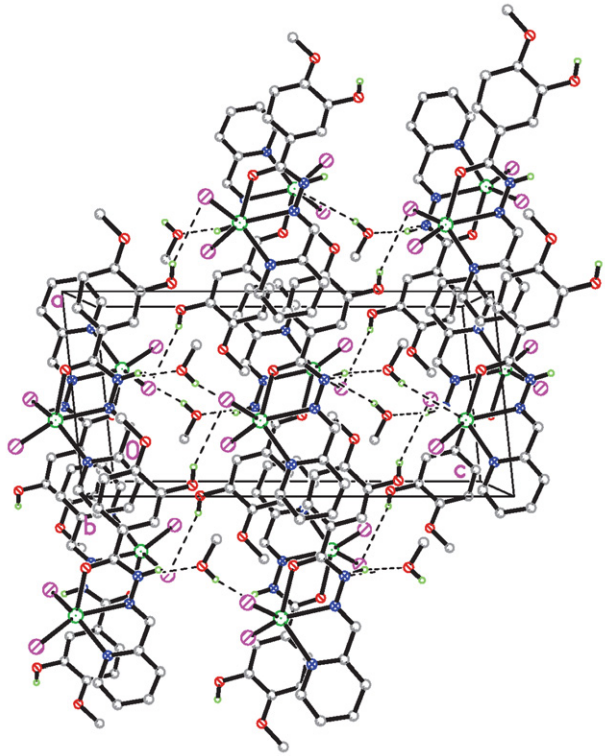

Fig. 4. Molecular packing diagram of complex **2**, viewed along the *b* axis. Hydrogen bonds are shown as dashed lines. H atoms not involved in hydrogen bonding are omitted for clarity.

3. 5. Structure Description of Complex 3

The molecular structure of complex **3** is shown in Fig. 5. The Zn atom is coordinated by two pyridine nitrogens (N3, N6), two imino nitrogens (N2, N5), and two enolate oxygens (O1, O2) from two hydrazone ligands, forming octahedral geometry. The octahedral coordination is distorted from the ideal model, which can be evidenced by the bond angles, ranging from 74.60(15) to 106.92(15)° for the *cis* angles, and from 146.64(14) to 177.60(16)° for the *trans* angles. The distortion arises from the strain created by the four five-membered chelate rings. The lengths of Zn–O bonds (2.141(3)-2.207(3) Å) and Zn–N bonds (2.052(4)-2.291(4) Å) are comparable to those observed in Schiff base zinc complexes with octahedral coordination.[23] The C1-C6 benzene ring and the C9-C13-N3 pyridine ring form a dihedral angle of 40.3(6)°. The C15-C20 benzene ring and the C23-C27-N6 pyridine ring form a dihedral angle of 18.3(6)°. In the crystal structure, the complex molecules are linked through intermolecular hydrogen

bonds of O–H···N, O–H···O, C–H···N and C–H···O, to form a three-dimensional network (Fig. 6).

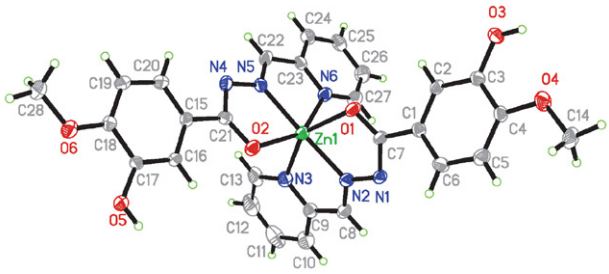

Fig. 5. Molecular structure of complex **3**. Displacement ellipsoids are drawn at the 30% probability level. Hydrogen bonds are shown as dashed lines.

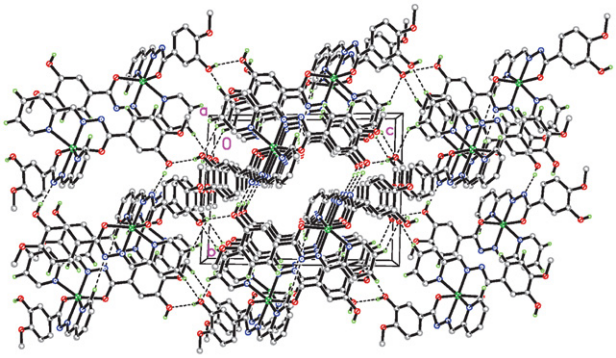

Fig. 6. Molecular packing diagram of complex **3**, viewed along the *a* axis. Hydrogen bonds are shown as dashed lines. H atoms not involved in hydrogen bonding are omitted for clarity.

Table 3. Hydrogen bond distances (Å) and bond angles (°) for the complexes

D–H···*A*	*d*(*D*–H)	*d*(H···*A*)	*d*(*D*···*A*)	Angle (*D*–H···*A*)
1				
O7–H7···N5$^{\#1}$	0.85(1)	2.57(4)	3.316(5)	147(6)
O7–H7···N4$^{\#1}$	0.85(1)	1.90(1)	2.749(5)	178(7)
O3–H3···O9	0.85(1)	1.83(3)	2.636(5)	159(6)
O9–H9A···O7$^{\#2}$	0.85(1)	1.90(2)	2.724(5)	163(6)
O5–H5···O1$^{\#3}$	0.85(1)	1.85(2)	2.671(4)	164(6)
O9–H9B···O8	0.87(1)	1.79(2)	2.621(8)	158(6)
C11–H11···O5$^{\#4}$	0.93	2.54(2)	3.074(7)	117(6)
C14–H14A···O2$^{\#5}$	0.96	2.39(2)	3.306(7)	160(6)
2				
N1–H1···O4	0.90(1)	1.87(3)	2.743(6)	162(8)
O4–H4···I2$^{\#6}$	0.82	3.29	3.869(7)	130(8)
O2–H2···I2$^{\#7}$	0.85(1)	3.09(4)	3.820(4)	146(6)
O2–H2···O3	0.85(1)	2.22(6)	2.649(6)	111(5)
3				
O3–H3···O5$^{\#8}$	0.85(1)	2.06(5)	2.828(5)	149(9)
O5–H5···N1$^{\#9}$	0.85(1)	1.84(2)	2.660(5)	161(5)
C13–H13···N4$^{\#10}$	0.93	2.55(2)	3.452(5)	165(5)
C19–H19···O1$^{\#11}$	0.93	2.60(2)	3.506(5)	165(5)
C25–H25···O3$^{\#12}$	0.9	2.49(2)	3.419(5)	173(5)
C26–H26···O3$^{\#13}$	0.93	2.48(2)	3.204(5)	135(5)

Symmetry codes: #1: –1/2 + *x*, 1/2 – *y*, 1 – *z*; #2: 1/2 + *x*, *y*, 1/2 – *z*; #3: 1 – *x*, 1 – *y*, 1 – *z*; #4: 3/2 – *x*, –1/2 + *y*, *z*; #5: –1/2 + *x*, *y*, 1/2 – *z*; #6: *x*, 1/2 – *y*, –1/2 + *z*; #7: –1 + *x*, 1/2 – *y*, –1/2 + *z*; #8: *x*, *y*, –1 + *z*; #9: 1 – *x*, 1 – *y*, 1 – *z*; #10: 2 – *x*, – *y*, 1 – *z*; #11: 1 – *x*, – *y*, 1 – *z*; #12: 2 – *x*, – *y*, – *z*; #13: 1 + *x*, *y*, *z*.

3. 6. Antibacterial Activities

The results of the antibacterial activities are given in Tables 4 and 5. All the complexes showed enhanced antibacterial activities as compared with the free Schiff base HL. Ciprofloxacin produced significantly sized inhibition zones against the bacteria, while DMSO produced no inhibitory effect against any of the tested organisms. HL gave inhibition zones in the range of 1.9–6.5 mm against the bacteria. The MIC results showed that complex **1** has weak activity against *Staphylococcus aureus* and *Pseudomonas aeruginosa*, and medium activity against *Bacillus subtilis* and *Escherichia coli*. Complex **2** has medium activity against *Staphylococcus aureus*, *Bacillus subtilis* and *Pseudomonas aeruginosa*, and strong activity agaisnt *Escherichia coli*. Complex **3** has good activity against *Staphylococcus aureus* and *Pseudomonas aeruginosa*, and strong activity against *Bacillus subtilis* and *Escherichia coli*. The results of this study agree well with those reported previously that metal complexes have higher activities than their precursors.[24] The overtone's concept[25] and Tweedy's chelation theory[26] can explain the enhanced in antibacterial activity of the metal complexes. In addition, the order of antibacterial activities is **3** (Zn) > **2** (Cd) > **1** (Ni), which may be caused by the different cellular uptake of the metal ions.

4. Conclusion

Three nickel(II), cadmium(II) and zinc(II) complexes derived from 3-hydroxy-4-methoxy-*N*'-[(*Z*)-(pyridin-2-yl)methylidene]benzohydrazide have been synthesized with microwave assisted heating method. Structures of the complexes have been confirmed by X-ray single crystal determination, which reveals that the Ni and Zn atoms in the nickel and zinc complexes are in octahedral coordination, and the Cd atom in the cadmium complex is in square pyramidal coordination. The biological activity assay indicates that the three complexes have enhanced antibacterial activities on the bacterial strains *Bacillus subtilis*, *Staphylococcus aureus*, *Pseudomonas aeruginosa* and *Escherichia coli* as compared to the free hydrazone ligand. The order of antibacterial activities is **3** (Zn) > **2** (Cd) > **1** (Ni). The zinc complex has the most antibacterial activity against *Escherichia coli* with MIC value of 4 μM, which deserves further study to explore new drugs.

Table 4. Diameter of growth of inhibition zone (mm)

Compounds	*Staphylococcus aureus*	*Bacillus subtilis*	*Escherichia coli*	*Pseudomonas aeruginosa*
HL	3.7	6.5	4.1	1.9
1	5.2	8.3	8.8	3.7
2	8.6	13.7	19.2	5.5
3	13.1	18.6	20.2	13.5
Ciprofloxacin	25.0	21.5	25.0	23.0
DMSO	0.27	0.23	0.12	0.15

Table 5. MIC values (μM)

Compounds	*Staphylococcus aureus*	*Bacillus subtilis*	*Escherichia coli*	*Pseudomonas aeruginosa*
HL	64	64	128	128
1	32	32	64	64
2	16	16	8	16
3	8	8	4	8
Ciprofloxacin	16	8	16	16
DMSO	>128	>128	>128	>128

Supplementary Materials

The X-ray crystallographic data in the CIF format for the structures of the complexes reported in this paper have been deposited with the Cambridge Crystallographic Data Center (CCDC: 2347408 (**1**), 2347409 (**2**) and 2347410 (**3**)) and the supplementary crystallographic data can be obtained free of charge on request at www.ccdc.cam.ac.uk/conts/retrieving.html [or from The Director, Cambridge Crystallographic Data Center, CCDC, 12 Union Road, Cambridge CB2 1EZ, UK; fax: +44(0)1223-336033; email: deposit@ccdc.cam.ac.uk], quoting the CCDC numbers 2249782-2249786.

Acknowledgments

This project was supported by the Qiqihar University.

5. References

1. (a) F. Nouali, J. L. C. Sousa, H. M. T. Albuquerque, R. F. Mendes, F. A. A. Paz, L. Saher, Z. Kibou, N. Choukchou-Braham, O. Talhi, A. M. S. Silva, *J. Mol. Struct.* **2023**, *1275*, 134608; **DOI:**10.1016/j.molstruc.2022.134608
(b) I. Gurgul, O. Mazuryk, D. Rutkowska-Zbik, M. Lomzik, A. Krasowska, P. Pietrzyk, G. Stochel, M. Brindell, *Polyhedron* **2022**, *225*, 116049; **DOI:**10.1016/j.poly.2022.116049
(c) E. Gabano, M. Ravera, *Molecules* **2022**, *27*, 4249; **DOI:**10.3390/molecules27134249
(d) A. J. Winstead, K. Alabrash, B. V. Powell, S. J. Parnell, T. V. Hinton, T. Odebode, J. N. Peng, J. A. Krause, P. Y. Zavalij, S. K. Mandal, *J. Organomet. Chem.* **2021**, *936*, 121718; **DOI:**10.1016/j.jorganchem.2021.121718
(e) R. A. Krishna, R. Dheepika, M. Muralisankar, S. Nagarajan, *J. Coord. Chem.* **2021**, *74*, 838–849. **DOI:**10.1080/00958972.2021.1885650
2. (a) S.-H. Zhang, Y.-L. Zhou, X.-J. Sun, L.-Q. Wei, M.-H. Zeng, H. Liang, *J. Solid State Chem.* **2009**, *182*, 2991–2996; **DOI:**10.1016/j.jssc.2009.08.009
(b) S.-H. Zhang, C. Feng, *J. Mol. Struct.* **2010**, *977*, 62–66. **DOI:**10.1016/j.molstruc.2010.05.010
3. (a) S. Bargujar, S. Ratnani, R. Jain, *Inorg. Chem. Commun.* **2024**, 112250; **DOI:**10.1016/j.inoche.2024.112250
(b) D. Karati, K. R. Mahadik, D. Kumar, *Curr. Microwave Chem.* **2022**, *9*, 99–104; **DOI:**10.2174/2213335609666220820153559
(c) S. Beniwal, A. Jain, N. Sharma, N. Fahmi, *J. Coord. Chem.* **2024**, *77*, 601–618. **DOI:**10.1080/00958972.2024.2330995
4. T. I. Kashar, S. S. Hassan, H. A. El-Boraey, *Inorg. Chim. Acta* **2024**, *563*, 121903. **DOI:**10.1016/j.ica.2023.121903
5. (a) Y.-T. Wang, X. Huang, X.-C. Cai, X.-X. Kang, H.-L. Zhu, *J. Mol. Struct.* **2024**, *1301*, 137343; **DOI:**10.1016/j.molstruc.2023.137343
(b) H. Kekecmuhammed, M. Tapera, E. Aydogdu, E. Saripinar, E. A. Karatas, E. M. Uc, M. Akyuz, B. Tuzun, I. Gulcin, R. E. Bora, I. O. Ilhan, *Chem. Biodivers.* **2023**, *20*; **DOI:**10.1002/cbdv.202200886
(c) K. Akdag, F. Tok, S. Karakus, O. Erdogan, O. Cevik, B. Kocyigit-Kaymakcioglu, *Acta Chim. Slov.* **2022**, *69*, 863–875. **DOI:**10.17344/acsi.2022.7614
6. M. S. Lone, M. M. Mubarak, S. A. Nabi, F. R. Wani, S. Amin, S. Nabi, H. A. Kantroo, M. Samim, S. Shafi, S. Ahmad, Z. Ahmad, S. O. Rizvi, K. Javed, *Med. Chem. Res.* **2023**, *32*, 808–826. **DOI:**10.1007/s00044-023-03039-5
7. (a) T. A. Farghaly, A. M. Al-Soliemy, R. Sabour, M. R. Shaaban, E. M. H. Abbas, *Bioorg. Chem.* **2022**, *121*, 105684;

DOI:10.1016/j.bioorg.2022.105684
(b) S. Jagetiya, P. S. Auti, A. T. Paul, *Chem. Biodivers.* **2023**, *20*; **DOI:**10.1002/cbdv.202301154
(c) M. Mollazadeh, H. Azizian, A. Fakhrioliaei, A. Iraji, L. Avizheh, Y. Valizadeh, K. Zomorodian, F. Elahi, A. Moazzam, H. Kazemzadeh, M. Amanlou, F. Garmciri, E. Hamidian, M. Biglar, B. Larijani, M. Mahdavi, *Med. Chem. Res.* **2023**, *32*, 930–943; **DOI:**10.1007/s00044-023-03050-w
(d) A. E. Evren, D. Nuha, S. Dawbaa, B. N. Saglik, L. Yurttas, *Eur. J. Med. Chem.* **2022**, *229*, 114097; **DOI:**10.1016/j.ejmech.2021.114097
(e) U. Salgin-Goksen, G. Telli, A. Erikci, E. Dedecengiz, B. C. Tel, F. B. Kaynak, K. Yelekci, G. Ucar, N. Gokhan-Kelekci, *J. Med. Chem.* **2021**, *64*, 1989–2009. **DOI:**10.1021/acs.jmedchem.0c01504

8. (a) H. Kargar, *Trans. Met. Chem.* **2014**, *39*, 811–817; **DOI:**10.1007/s11243-014-9863-4
(b) A. Sahraei, H. Kargar, M. Hakimi, M. N. Tahir, *J. Mol. Struct.* **2017**, *1149*, 576–584; **DOI:**10.1016/j.molstruc.2017.08.022
(c) A. Sahraei, H. Kargar, M. Hakimi, M. N. Tahir, *Trans. Met. Chem.* **2017**, *42*, 483–489; **DOI:**10.1007/s11243-017-0152-x
(d) A. Jamshidvand, M. Sahihi, V. Mirkhani, M. Moghadam, I. Mohammadpoor-Baltork, S. Tangestaninejad, H. A. Rudbari, H. Kargar, R. Keshavarzi, S. Gharaghani, *J. Mol. Liquids* **2018**, *253*, 61–71; **DOI:**10.1016/j.molliq.2018.01.029
(e) H. Kargar, R. Behjatmanesh-Ardakani, V. Torabi, M. Kashani, Z. Chavoshpour-Natanzi, Z. Kazemi, V. Mirkhani, A. Sahraei, M. N. Tahir, M. Ashfaq, K. S. Munawar, *Polyhedron* **2021**, *195*, 114988; **DOI:**10.1016/j.poly.2020.114988
(f) H. Kargar, F. Aghaei-Meybodi, R. Behjatmanesh-Ardakani, M. R. Elahifard, V. Torabi, M. Fallah-Mehrjardi, M. N. Tahir, M. Ashfaq, K. S. Munawar, *J. Mol. Struct.* **2021**, *1230*, 129908; **DOI:**10.1016/j.molstruc.2021.129908
(g) H. Kargar, A. A. Ardakani, M. N. Tahir, M. Ashfaq, K. S. Munawar, *J. Mol. Struct.* **2021**, *1233*, 130112. **DOI:**10.1016/j.molstruc.2021.130112
9. M. Orojloo, P. Zolgharnein, M. Solimannejad, S. Amani, *Inorg. Chim. Acta* **2017**, *467*, 227–237. **DOI:**10.1016/j.ica.2017.08.016
10. (a) B. Ay, O. Sahin, B. S. Demir, Y. Saygideger, J. M. Lopez-de-Luzuriaga, G. Mahmoudi, D. A. Safin, *New J. Chem.* **2020**, *44*, 9064–9072; **DOI:**10.1039/D0NJ00921K
(b) K. S. Neethu, S. Sivaselvam, M. Theetharappan, J. Ranjitha, N. S. P. Bhuvanesh, N. Ponpandian, M. A. Neelakantan, M. V. Kaveri, *Inorg. Chim. Acta* **2021**, *524*, 120419; **DOI:**10.1016/j.ica.2021.120419
(c) G. A. El-Inany, H. S. Seleem, H. F. El-Shafiy, B. A. El-Shetary, A. I. Nabeel, A. Madyan, M. Shebl, *Appl. Organomet. Chem.* **2024**, *38*; **DOI:**10.1002/aoc.7367
(d) A. A. Khandar, Z. M. Azar, M. Eskandani, C. B. Hubschle, S. van Smaalen, B. Shaabani, Y. Omidi, *Polyhedron* **2019**, *171*, 237–248; **DOI:**10.1016/j.poly.2019.06.026
(e) P. H. O. Santiago, M. B. Santiago, C. H. G. Martins, C. C. Gatto, *Inorg. Chim. Acta* **2020**, *508*, 119632; **DOI:**10.1016/j.ica.2020.119632
(f) S. Dasgupta, S. Karim, S. Banerjee, M. Saha, K. D. Saha, D. Das, *Dalton Trans.* **2020**, *49*, 1232–1249; **DOI:**10.1039/C9DT04636D
(g) Y.-L. Sang, X.-S. Lin, W.-D. Sun, *Acta Chim. Slov.* **2020**, *67*, 581–585. **DOI:**10.17344/acsi.2019.5595
11. (a) W.-G. Zhang, *Acta Chim. Slov.* **2023**, *70*, 421–429; **DOI:**10.17344/acsi.2023.8144
(b) W.-G. Zhang, J.-H. Liang, *Acta Chim. Slov.* **2021**, *68*, 921–929. **DOI:**10.17344/acsi.2021.6902
12. Siemens, SAINT: Area Detector Control and Integration Software, Siemens Analytical X-ray Instruments Inc., Madison, WI, USA, **1996**.
13. G. M. Sheldrick, SHELXL97 and SHELXTL Software Reference Manual, Version 5.1, Brucker AXS Inc., Madison, WI, USA, **1997**.
14. G. M. Sheldrick, SADABS, University of Göttingen, Germany, **1996**.
15. K. Singh, Y. Kumar, P. Puri, C. Sharma, K. R. Aneja, *Med. Chem. Res.* **2012**, *21*, 1708–1716. **DOI:**10.1007/s00044-011-9683-4
16. M. I. Okeke, C. U. Iroegbu, E. N. Eze, A. S. Okoli, C. O. Esimone, *J. Ethnopharmacol.* **2001**, *78*, 119–127. **DOI:**10.1016/S0378-8741(01)00307-5
17. G. Kastas, C. A. Kastas, A. Tabak, *Spectrochim. Acta A* **2019**, *222*, 117198.
18. M.-L. Liu, J.-M. Dou, J.-Z. Cui, D.-C. Li, D.-Q. Wang, *J. Mol. Struct.* **2012**, *1011*, 140–144. **DOI:**10.1016/j.molstruc.2011.12.024
19. A. A. El-Sherif, A. Fetoh, Y. K. Abdulhamed, G. M. Abu El-Reash, *Inorg. Chim. Acta* **2018**, *480*, 1–15. **DOI:**10.1016/j.ica.2018.04.038
20. (a) R. N. Patel, A. Singh, V. P. Sondhiya, Y. Singh, K. K. Shukla, D. K. Patel, R. Pandey, *J. Coord. Chem.* **2012**, *65*, 795–812; **DOI:**10.1080/00958972.2012.662592
(b) P. Sathyadevi, P. Krishnamoorthy, M. Alagesan, K. Thanigaimani, P. T. Muthiah, N. Dharmaraj, *Polyhedron* **2012**, *31*, 294–306; **DOI:**10.1016/j.poly.2011.09.021
(c) C. M. Armstrong, P. V. Bernhardt, P. Chin, D. R. Richardson, *Eur. J. Inorg. Chem.* **2003**, 1145–1156. **DOI:**10.1002/ejic.200390146
21. A. W. Addison, T. N. Rao, J. Reedijk, J. van Rijn, G. C. Verschoor, *J. Chem. Soc., Dalton Trans.* **1984**, *7*, 1349–1356. **DOI:**10.1039/DT9840001349
22. (a) L.-X. Xie, D.-Y. Wu, C.-Y. Duan, B.-G. Zhang, Q.-J. Meng, *Chin. J. Inorg. Chem.* **2007**, *23*, 191–199;
(b) K. Das, T. N. Mandal, S. Roy, S. Gupta, A. K. Gupta, A. K. Barik, P. Mitra, A. L. Rheingold, S. K. Kar, *Polyhedron* **2010**, *29*, 2892–2899. **DOI:**10.1016/j.poly.2010.07.015
23. (a) P. Barbazan, R. Carballo, E. M. Vazquez-Lopez, *CrystEngComm* **2007**, *9*, 668–675; **DOI:**10.1039/b703442c
(b) B. Samanta, J. Chakraborty, S. Shit, S. R. Batten, P. Jensen, J. D. Masuda, S. Mitra, *Inorg. Chim. Acta* **2007**, *360*, 2471–2484. **DOI:**10.1016/j.ica.2006.12.019
24. K. Singh, Y. Kumar, P. Puri, M. Kumar, C. Sharma, *Eur. J. Med. Chem.* **2012**, *52*, 313–321. **DOI:**10.1016/j.ejmech.2012.02.053

25. N. Raman, A. Kulandaisamy, K. Jayasubramanian, *Polish J. Chem.* **2002**, *76*, 1085–1094.

26. B. G. Tweedy, *Phytopathology* **1964**, *55*, 910–915.

Povzetek

Z uporabo mikrovalovne metode smo sintetizirali tri komplekse z ligandom 3-hidroksi-4-metoksi-*N*'-[(*Z*)-(piridin-2-il) metiliden]benzohidrazid (HL): $[NiL_2]\cdot 2CH_3OH\cdot H_2O$ (**1**), $[CdI_2(HL)]\cdot CH_3OH$ (**2**) in $[ZnL_2]$ (**3**). Vse spojine smo karakterizirali s CHN elementno analizo in infrardečo spektroskopijo. Strukture kompleksov smo določili z monokristalno rentgensko difrakcijo, ki je pokazala, da sta atoma Ni in Zn v spojinah **1** in **3** oktaedrično koordinirana, medtem ko je atom Cd v spojini **2** kvadratno piramidalno koordiniran. Biološko aktivnost kompleksov smo preverili na bakterijskih sevih *Bacillus subtilis*, *Staphylococcus aureus*, *Pseudomonas aeruginosa* in *Escherichia coli*. Izkazalo se je, da ima predvsem cinkov kompleks zanimivo antibakterijsko učinkovitost.